

Study and Analysis of Calcium Substitution in $Y_{0.8}Pr_{0.2}Ba_2Cu_3O_{7-\Delta}$

Rashmi Meel ; Dr.Amit Kumar ,Dr.Sumit Kumar Gupta

¹ Research Scholar, Sunrise University, Alwar, Rajasthan, India

²Professor, Department of Physics, Sunrise University, Alwar Rajasthan, India

³Professor, Department of Physics, Parishkar College of Global Excellence, Jaipur, Rajasthan, India

ABSTRACT:

YBa₂Cu₃O_{7-δ} cuprate is a suitable system for the study of impurity effect on superconducting properties because carrier concentration can be widely changed without introducing significant disorder. Thus, the effect of replacing Cu by Co atoms, and Y by Ca atoms is reported to provide useful information about the mechanism of high-T_c superconductivity. In this paper, we have investigated the effect of Ca and Co simultaneous substitution on the structural and physical properties for a series of (Y_{1-x}Ca_x)Ba₂(Cu_{0.98}Co_{0.02})₃O_{7-δ} (0 ≤ x ≤ 0.35) ceramic. Doped Y123 samples are prepared by conventional solid-state reaction method and characterized by X-ray diffraction (XRD), SEM, and resistivity measurements. We found that the obtained crystalline structure is mainly orthorhombic. No parasite phase is observed. The orthorhombicity increases with Ca content. The analysis of the superconducting behavior of the samples showed that co-substitution of Ca does not counteract the adverse influence of Co within the single-phase range

Introduction

INTRODUCTION

SAMPLE PREPARATION

The preparation method of the substitutions of 5% to 25% Ca, with a constant 20% Pr, into $Y_{0.8}Pr_{0.2}Ba_2Cu_3O_{7-\delta}$ is different from the Pr substituted samples and thus a 0% Ca substituted sample is included as a

comparison for the previous set of measurements. Mixed powders of $(Y_{0.8-y}Pr_{0.2}Ca_y)Ba_2Cu_3O_{7-\delta}$ for the concentrations of y = 0.05, 0.1, 0.15, 0.2, and 0.25 were calcined in air at 905°C for a total of 125 hours with several intermediate regrindings to improve the homogeneity of the samples. The sintering process was performed in the parallel processing system and consisted of the following heat treatment:

1. heat to 935°C holding for 48 hours; then and
2. cool to 500°C and hold for 18 hours; then
3. cool to 400°C and hold for 10 hours; then
4. cool to 300°C and hold for 10 hours; then
5. cool to room temperature.

All sintering cooling processes were at the natural cooling rate of the oven.

Resistance measurements were performed on the pellets and then shaped rods and bars were made from the pellets. Magnetization, both ZFC and FC data, were performed on the rods and resistivity measurements were performed on the bars.

MEASUREMENTS

A comparison of the dc magnetization, the ZFC and FC curves, is given in Figure 1. The Meissner fractions are tabulated in Table 1 along with the transition widths calculated

(as described earlier) from the ac susceptibility (Figure 2), and resistivity (Figure 3) measurements. A characteristic comparison (10% Ca) for the Ca substitution

series of all three measurements is given in Figure 4. The Ca samples also exhibit the small (< 3%) BaCuO₂ impurities that was seen in the Pr X- ray measurements.

Ca concentration (at.%)	¹⁸ O concentration (at.%)	Meissner Fraction @0.05Oe	Transition Width (K)		
			Mag.	Susc.	Res.
0	(85)	35%	5.2	3.7	2.5
5	84	16%	2.0	1.4	1.3
10	78	12%	1.0	0.9	0.8
15	77	17%	1.9	1.5	1.0
20	76	21%	2.0	1.6	1.0
25	75	24%	1.7	1.4	1.3

Table 1. General characteristics of Ca substituted Y(20%Pr)BCO. A number in parenthesis indicates that this value is an estimate.

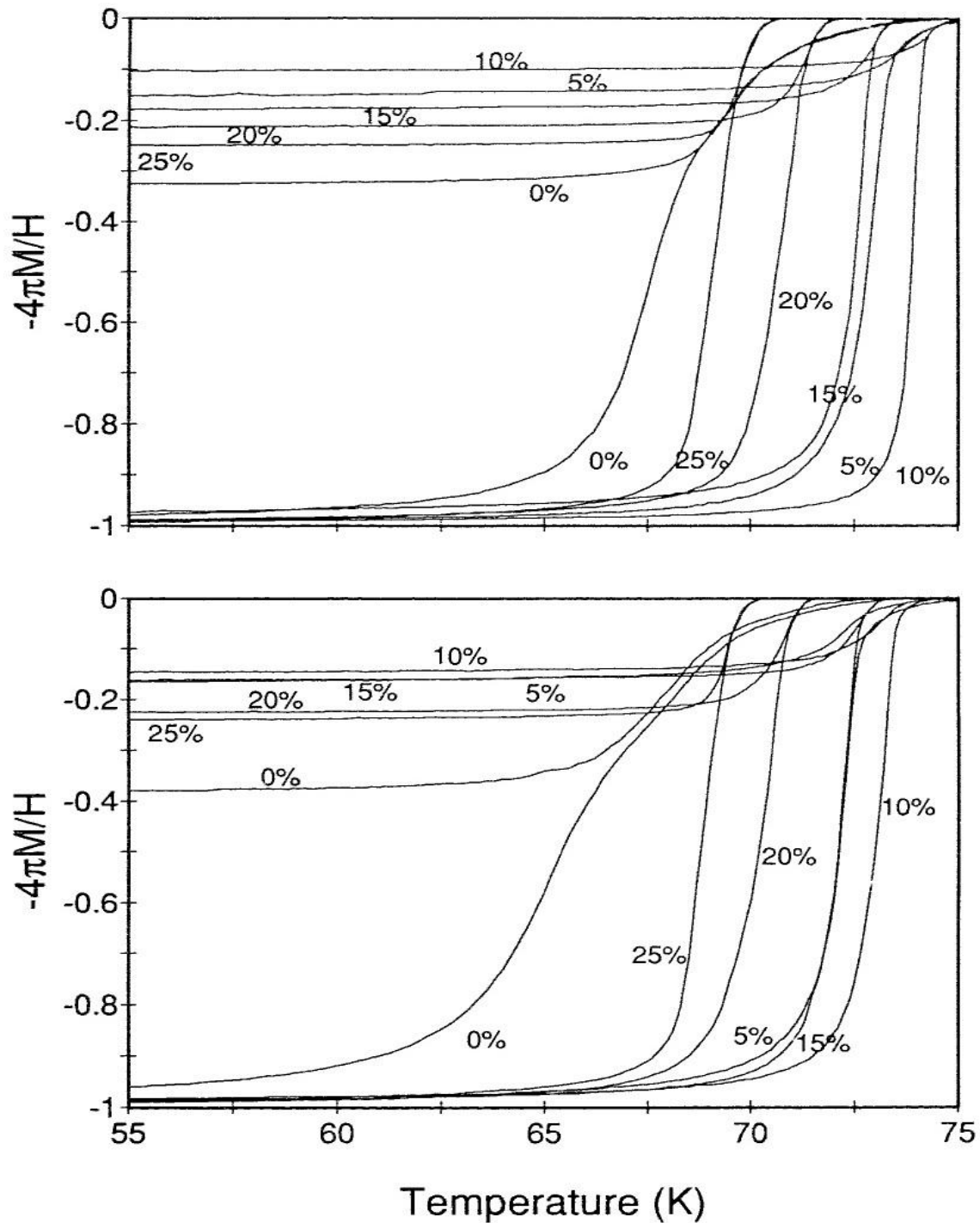


Figure 1

DC magnetization vs. temperature for Ca substituted Y(20% Pr)BCO. Top ^{16}O data; Bottom ^{18}O data. Both the ZFC and FC data are shown giving the Meissner fraction.

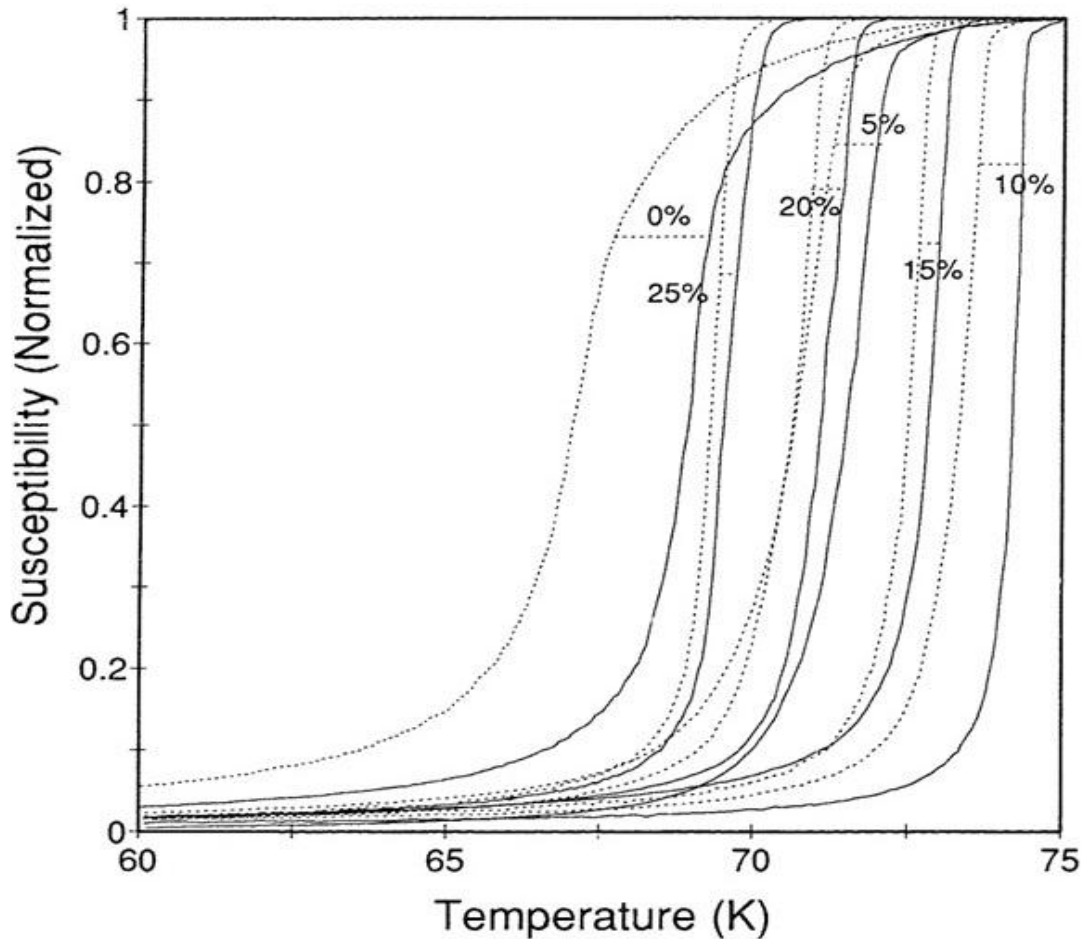


Figure 2

AC susceptibility vs. temperature for Ca substituted Y(20% Pr)BCO. Solid lines represent the ^{16}O isotope data and the dashed lines represent the ^{18}O isotope data. A dashed lines represent the ^{18}O pairs is to help distinguish the curves.

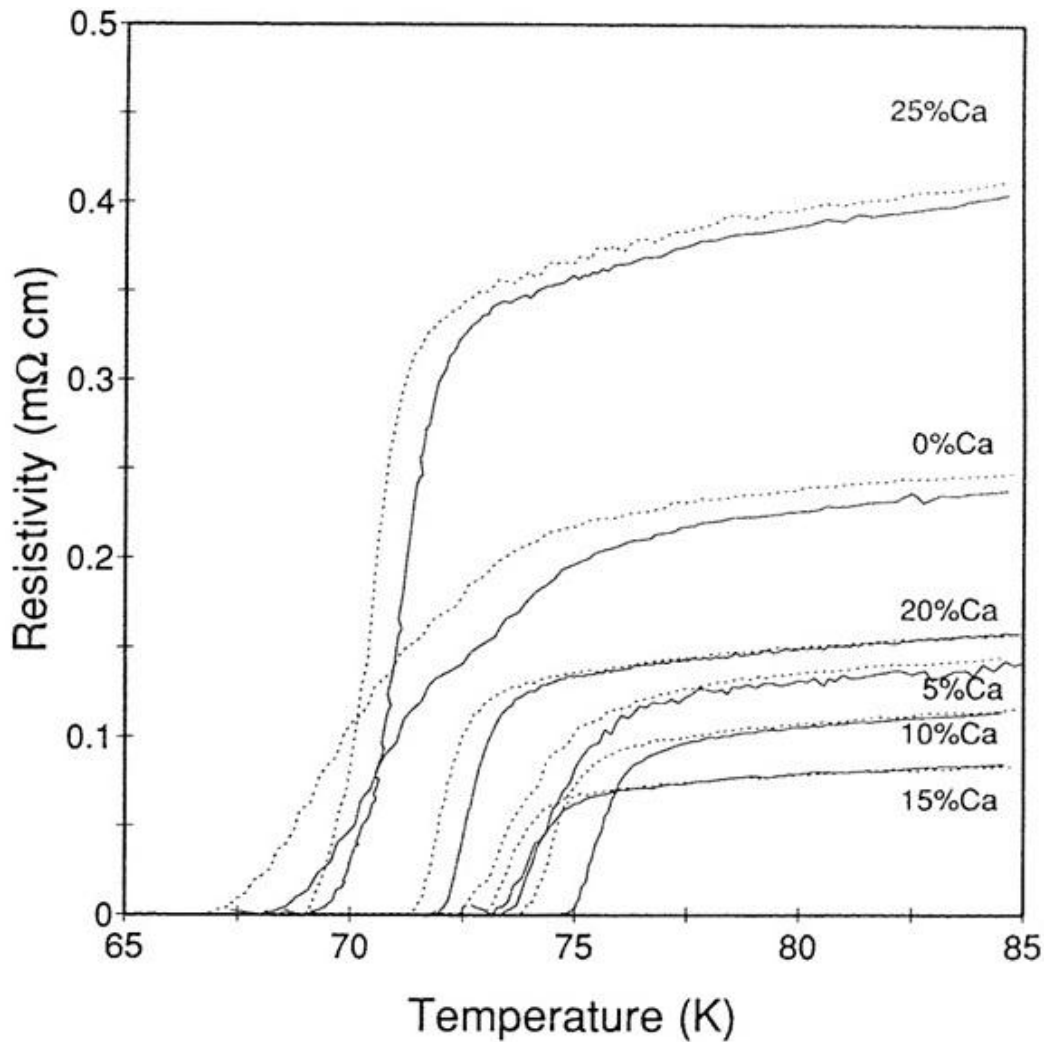


Figure 3

DC resistivity vs. temperature for Ca substituted Y(20% Pr)BCO. The solid lines represent the ^{16}O isotope data and the dashed lines represent the ^{18}O isotope data

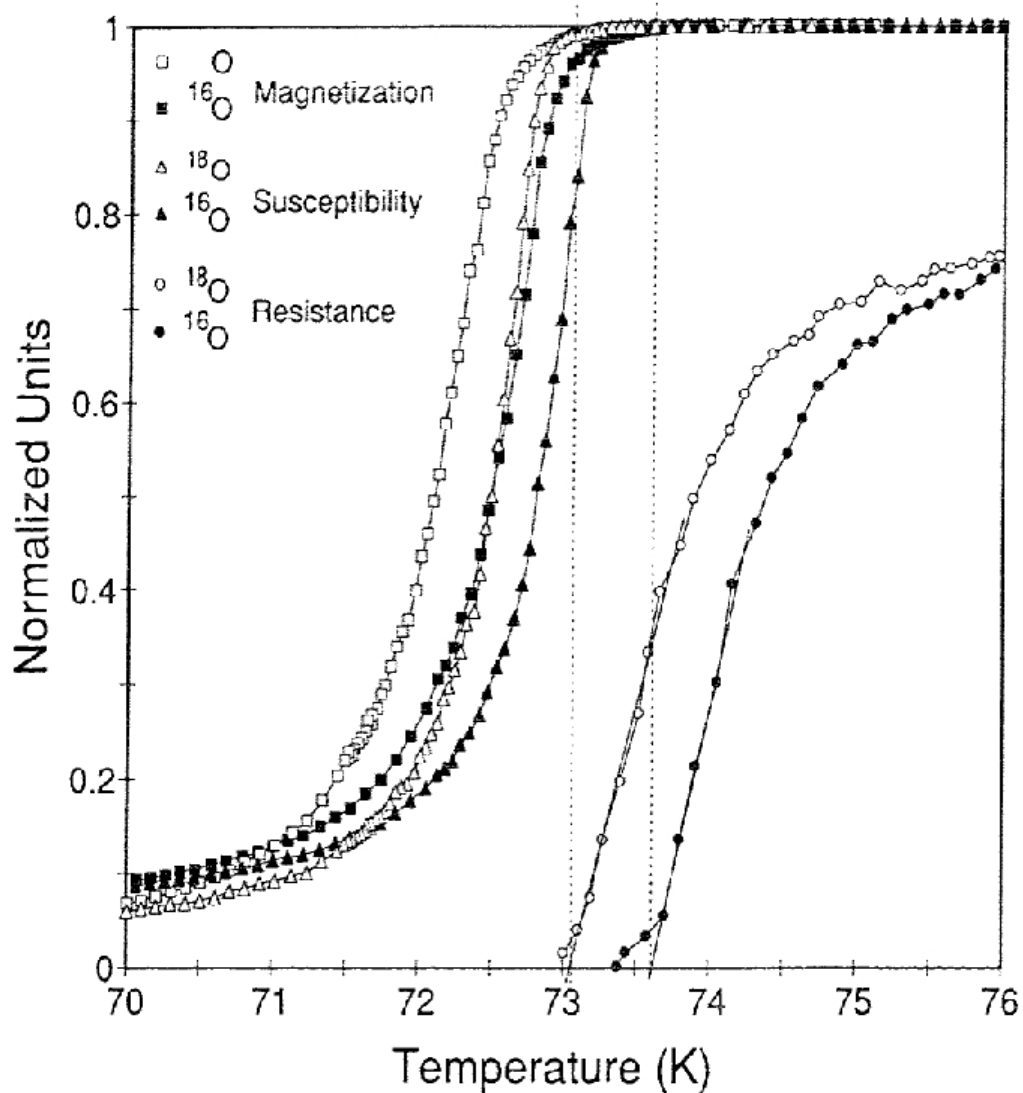


Figure 4

Comparison of dc magnetization, ac susceptibility and resistance measurements for $Y_{0.8}Pr_{0.2}Ba_2Cu_3O_{7-\delta}$. The symbols represent the data. The solid lines provide continuity from point to point. The dotted lines are a visual aid for the critical

temperature of the resistive transition (obtained from the straight, line extrapolation). The resistive transition was normalized to $R(85K)$.

The obvious effect of the addition of Ca is an increase in the sharpness of the transition, and the elimination of the long tails at very small shielding. The width of the transition sharpness for all three measurements with the

additions of Ca and remains fairly constant with the increasing Ca concentration. As with the Pr, the resistance has the narrowest transition and the for dc magnetization has the widest. The isotopic shift measured is similar for both magnetic measurement but the resistivity measurement give a somewhat larger value for the higher concentration .the size of the isotopic shift is affected also by the addition of Ca as it is reduced from that of the 20% Pr sample fabricated under the same conditions. The reductions is considerable since the change in T_c is quite small only about 7K throughout the entire substitution range The increase in Ca concentration in the sample has an effect on a number of properties of this system. First, T_c increase then decrease with a maximum at approx. 10% Ca. Second, the Meissner fraction decrease then increase with a minimum at the

10% Ca. The normal state resistivity (at $T=85K$) is also parabolically dependent on the Ca concentration although its minimum is the slightly higher concentration. The parabolic effect in T_c (Figure 5) has been reported earlier The T_c data and the corresponding concentration of both the Pr, x, and the Pr:Ca, y, series has been fitted to the function proposed by Neumeier et al⁵⁹. The dotted line in Figure 5 indicates this fit to equation [2.1], which gives:

$$T_c(x,y) = 93.6K - (157K)(0.091-0.874x+y)^2 - (93.3K)x \quad [1]$$

It should be noted that the last in equation [1], the linear pair-Breaking term, is an approximation to the more complicates digamma function which

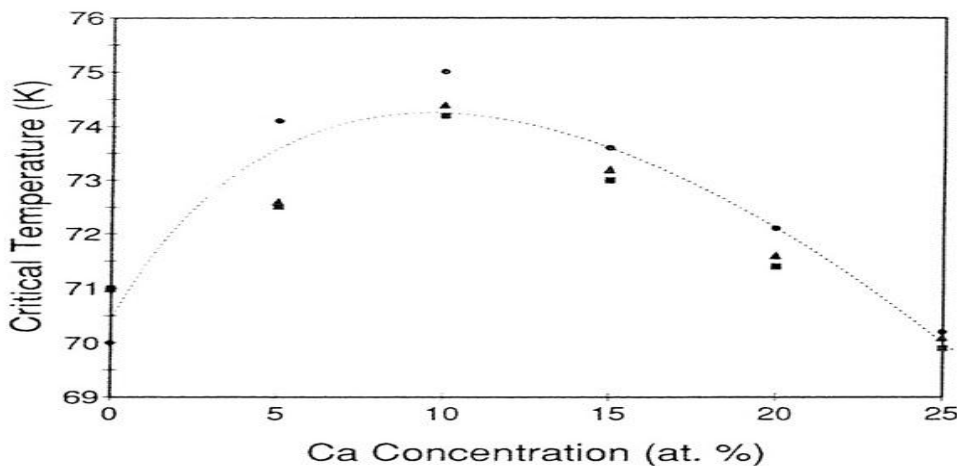


Figure 5

Critical temperature vs. Ca concentration. The parabolic line is a fit of the data to the function⁷³ $T_c(x,y) = T_{co}-A(\gamma-\beta x-y)^2-Bx$, where x is the Pr concentration and y is the Ca concentration. We obtain $T_{co} = 93.6K$, $a=157K$, $B= 93.3K$, $\gamma=0.091$, and $\beta=0.874$. Both the Pr and the Pr:Ca data is used in

fitting the function. should be used when dealing with the highest Pr concentrations because the pair-breaking here is no longer linear.

The data, the Simplex fit to the data, and the computed isotope shift for the system of $(Y_{0.8}Pr_{0.2}Ba_2Cu_3O_{7-\delta})$, $y = 0, 0.05, 0.1, 0.15, 0.2, 0.25$, is given in Figures 6 to 11

respectively. The critical temperatures, the isotope shifts, and the computed values of the isotope coefficient for this system are given in Table 2. The relationship between α and ΔT_c as a function of T_c is given in Figure 12. Due to the smaller temperature range plotted here, the uncertainty in the temperature values appear large. In fact, they are actually smaller than that obtained in the Pr series. The value of T_c reported in the table is that which has been determined from the linear extrapolation technique as explained earlier. The isotopic shift, ΔT_c and the value of the isotope coefficient, α , change little over the short spread in critical temperature. The relationship between the critical temperature and α or ΔT_c is not clear. Considering the parabolic nature of the other properties of the system, a possible parabolic fit to α and ΔT_c , can be detected in the data (dotted line Figure 12). However, the large relative uncertainties also leave the possibility that of a linear

relationship or perhaps even no change in ΔT_c at all. The empty symbols represent the ^{18}O data and the filled symbols represent the ^{16}O data. The solid line represents the Simplex fit to the data. The "+" symbols represent the shift, ΔT_i , as a function of temperature, between the two fits to the data. The arrows on the magnetization and susceptibility graphs indicate the critical temperature obtained from a linear extrapolation of the bulk of the transition: 71.0K for both the magnetization and susceptibility. The upper limit for T_c is 76.0 K.

The vertical dotted line (magnetic measurements) indicates the cutoff in the calculation of the mean of the isotope shift. The horizontal line indicates this mean, and its value is indicated above the line. The resistance measurements are normalized to $R(85\text{K})$. Not all temperature scales are equivalent.

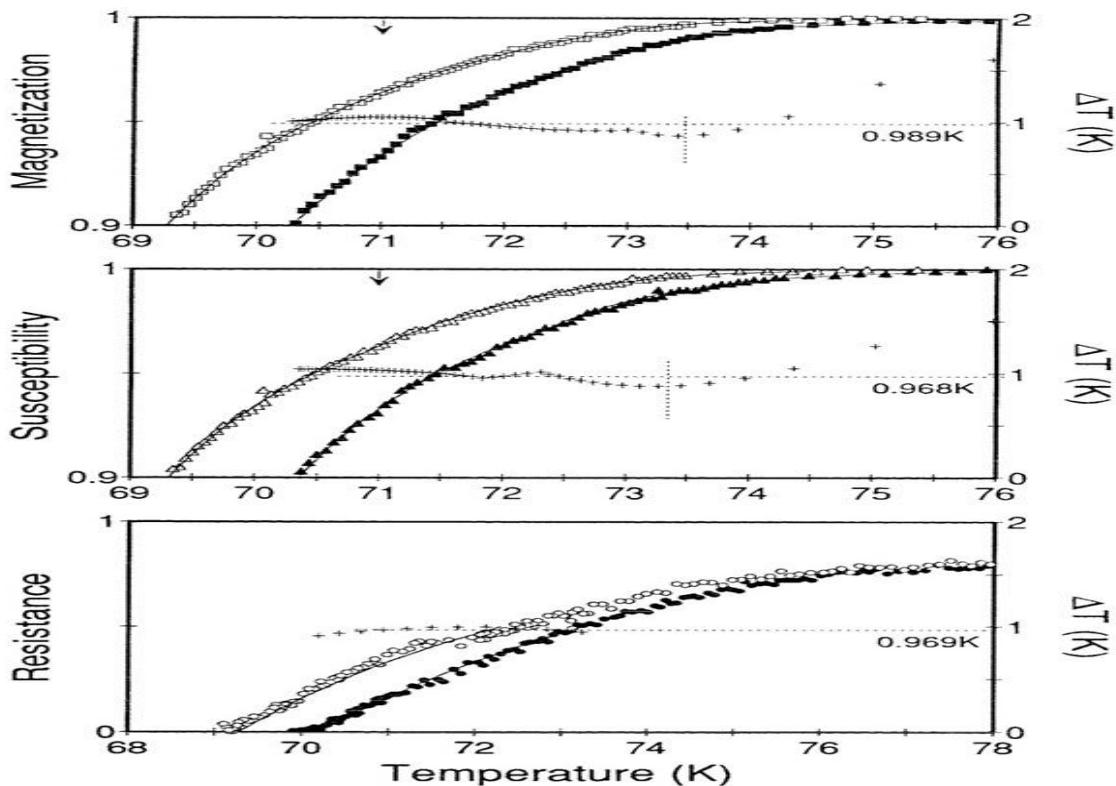


Figure 6 Oxygen isotope effect in $(Y_{0.8}Pr_{0.2})Ba_2Cu_3O_{7-\delta}$, 0% Ca, 20% Pr substitution

The empty symbols represent the ^{18}O data and the filled symbols represent the ^{16}O data. The solid line represents the Simplex fit to the data. The "+" symbols represent the shift, ΔT_i , as a function of temperature, between the two fits to the data. The arrows on the magnetization and susceptibility graphs indicate the critical temperature obtained from a linear extrapolation of the bulk of the

transition: 72.5K for the magnetization (upper limit = 74.8K) and 72.6K for the susceptibility (upper limit = 74.6K). No cutoff was imposed in the calculation of the mean of the isotope shift. The horizontal line indicates this mean, and its value is indicated above the line. The resistance measurements are normalized to $R(85K)$. Not all temperature scales are equivalent.

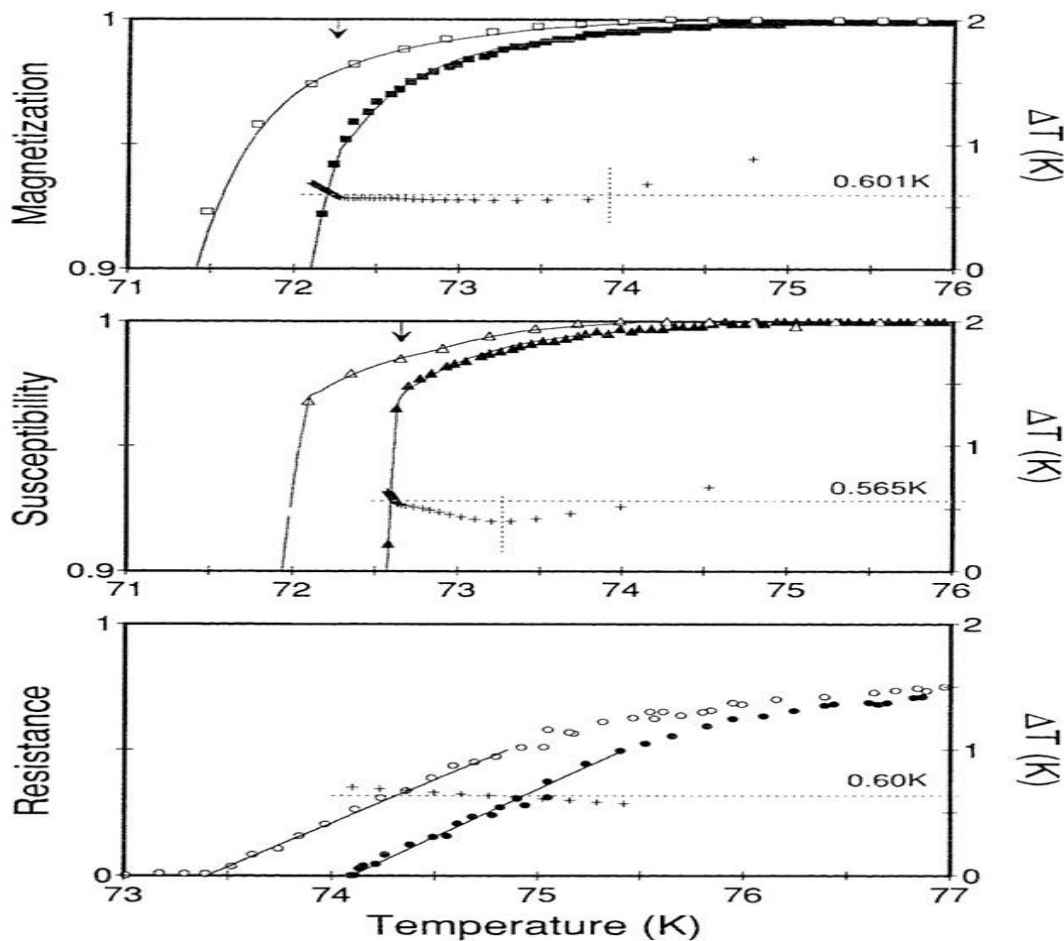


Figure 7 Oxygen isotope effect in $(Y_{0.8}Pr_{0.2}Ca_{0.05})Ba_2Cu_3O_{7-\delta}$, 5% Ca, 20% Pr substitution

The empty symbols represent the ^{18}O data and the filled symbols represent the ^{16}O data. The solid line represents the Simplex fit to the

data. The "+" symbols represent the shift, ΔT_i , as a function of temperature, between the two fits to the data.

The arrows on the magnetization and susceptibility graphs indicate the critical temperature obtained from a linear extrapolation of the bulk of the transition: 74.2K for the magnetization (upper limit = 75.8K) and 74.4K for the susceptibility (upper limit = 75.7K). No cutoff was imposed

in the calculation of the mean of the isotope shift. The horizontal line indicates this mean, and its value is indicated above the line. The resistance measurements are normalized to R(85K).

Not all temperature scales are equivalent.

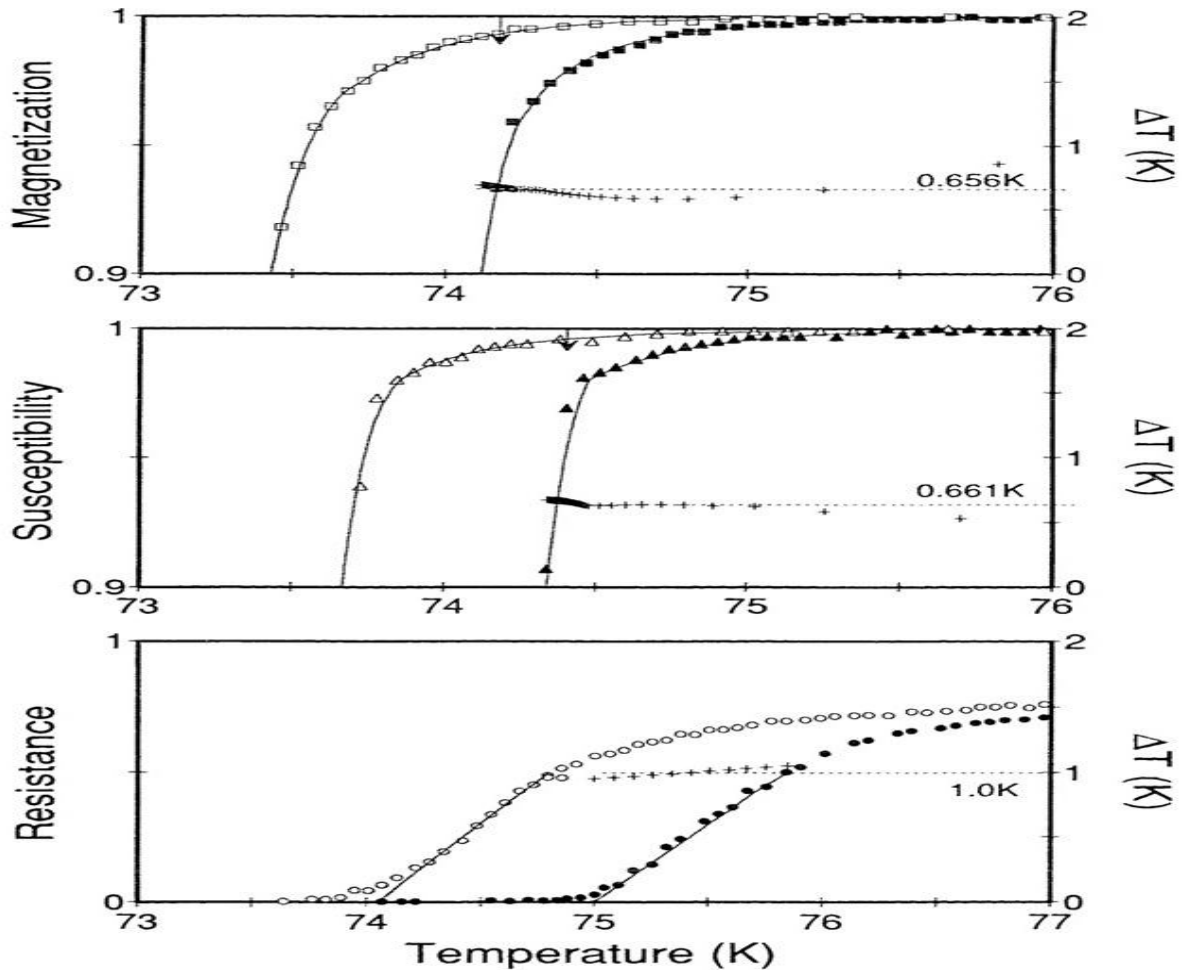


Figure 8 Oxygen isotope effect in $(Y_{0.8}Pr_{0.2}Ca_{0.1})Ba_2Cu_3O_{7-\delta}$, 10% Ca, 20% Pr substitution

ΔT_i as a function of temperature, between the two fits to the data.

The empty symbols represent the ^{18}O data and the filled symbols represent the ^{16}O data. The solid line represents the Simplex fit to the data. The "+" symbols represent the shift,

The arrows on the magnetization and susceptibility graphs indicate the critical temperature obtained from a linear extrapolation of the bulk of the transition: 73.0K for the magnetization (upper limit = 74.0K) and 73.2K for the susceptibility (upper limit = 73.8K). No cutoff was imposed in the

calculation of the mean of the isotope shift. The horizontal line indicates this mean, and its value is indicated above the line. The

resistance measurements are normalized to R(85K).

Not all temperature scales are equivalent.

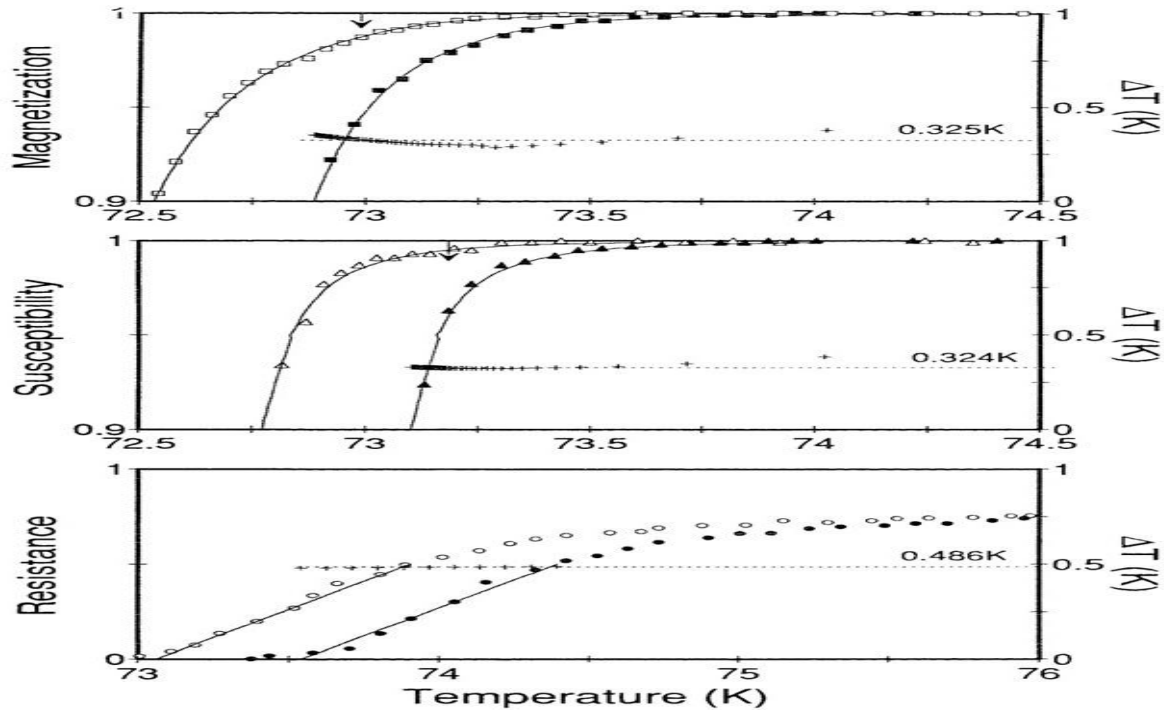


Figure 9 Oxygen isotope effect in $(Y_{0.65}Pr_{0.2}Ca_{0.15})Ba_2Cu_3O_{7-\delta}$, 15% Ca, 20% Pr substitution

The empty symbols represent the ^{18}O data and the filled symbols represent the ^{16}O data. The solid line represents the Simplex fit to the data. The "+" symbols represent the shift, ΔT_i , as a function of temperature, between the two fits to the data. The arrows on the magnetization and susceptibility graphs

indicate the critical temperature obtained from a linear extrapolation of the bulk of the transition: 71.4K for the magnetization (upper limit = 72.54 and 71.6K for the susceptibility (upper limit = 72.6K). No cutoff was imposed in the calculation of the mean of the isotope shift. The horizontal line indicates this mean, and its value is indicated above the line. The resistance measurements are normalized to R(85K). Not all temperature scales are equivalent.

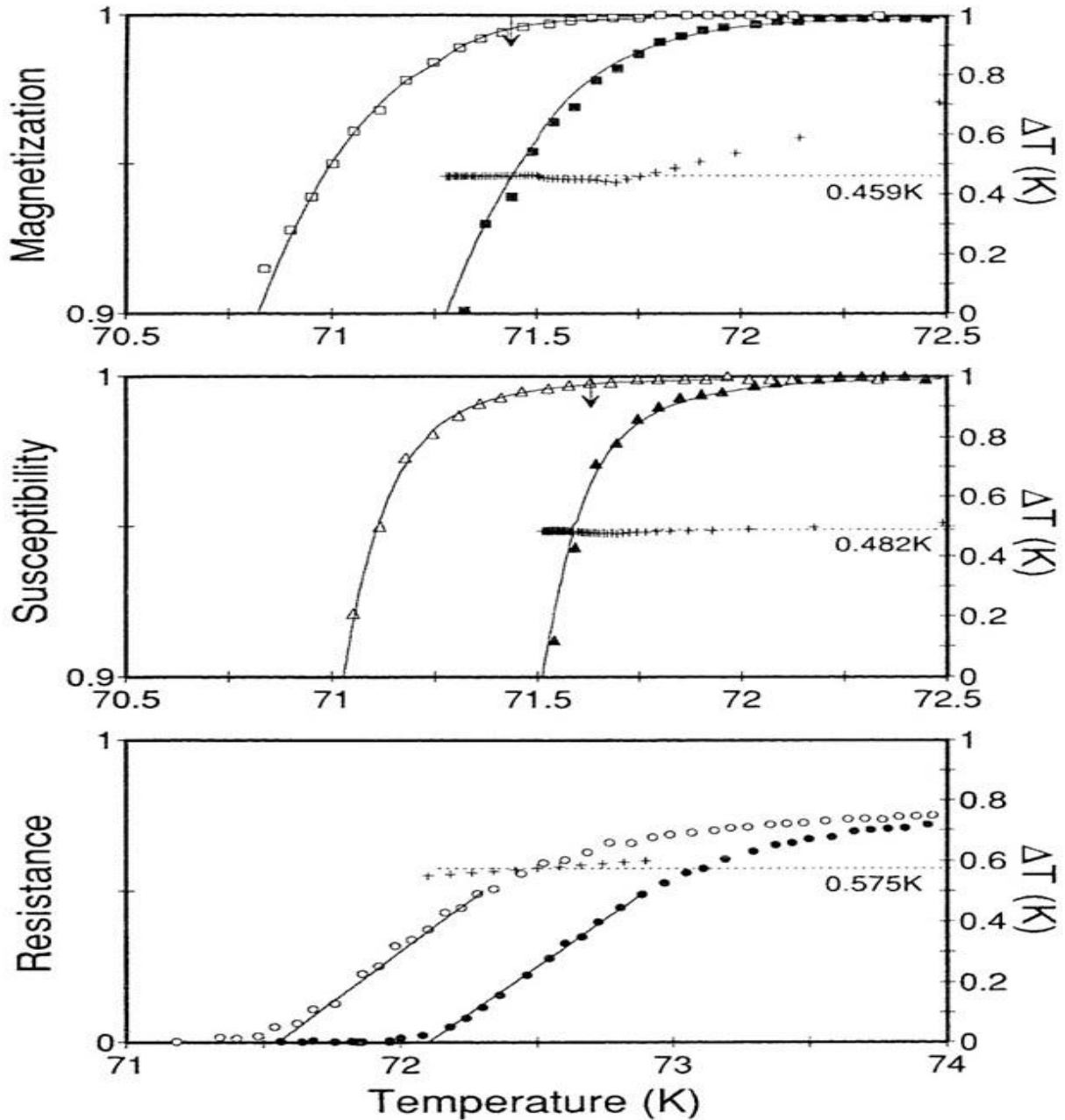


Figure 10 Oxygen isotope effect in ($Y_{0.6}Pr_{0.2}Ca_{0.2}Ba_2Cu_3O_{7-\delta}$), 0% Ca, 20% Pr substitution

The empty symbols represent the ^{18}O data and the filled symbols represent the ^{16}O data. The solid line represents the Simplex fit to the data. The "+" symbols represent the shift, ΔT_i : as a function of temperature, between the two fits to the data. The arrows on the

magnetization and susceptibility graphs indicate the critical temperature obtained from a linear extrapolation of the bulk of the transition: 69.9K for the magnetization (upper limit = 70.9K) and 70.1K for the susceptibility (upper limit = 71.2K). No cutoff was imposed in the calculation of the

mean of the isotope shift. The horizontal fine indicates this mean, and its value is indicated above the line.

The resistance measurements are normalized to R(85K). Not all temperature scales are equivalent.

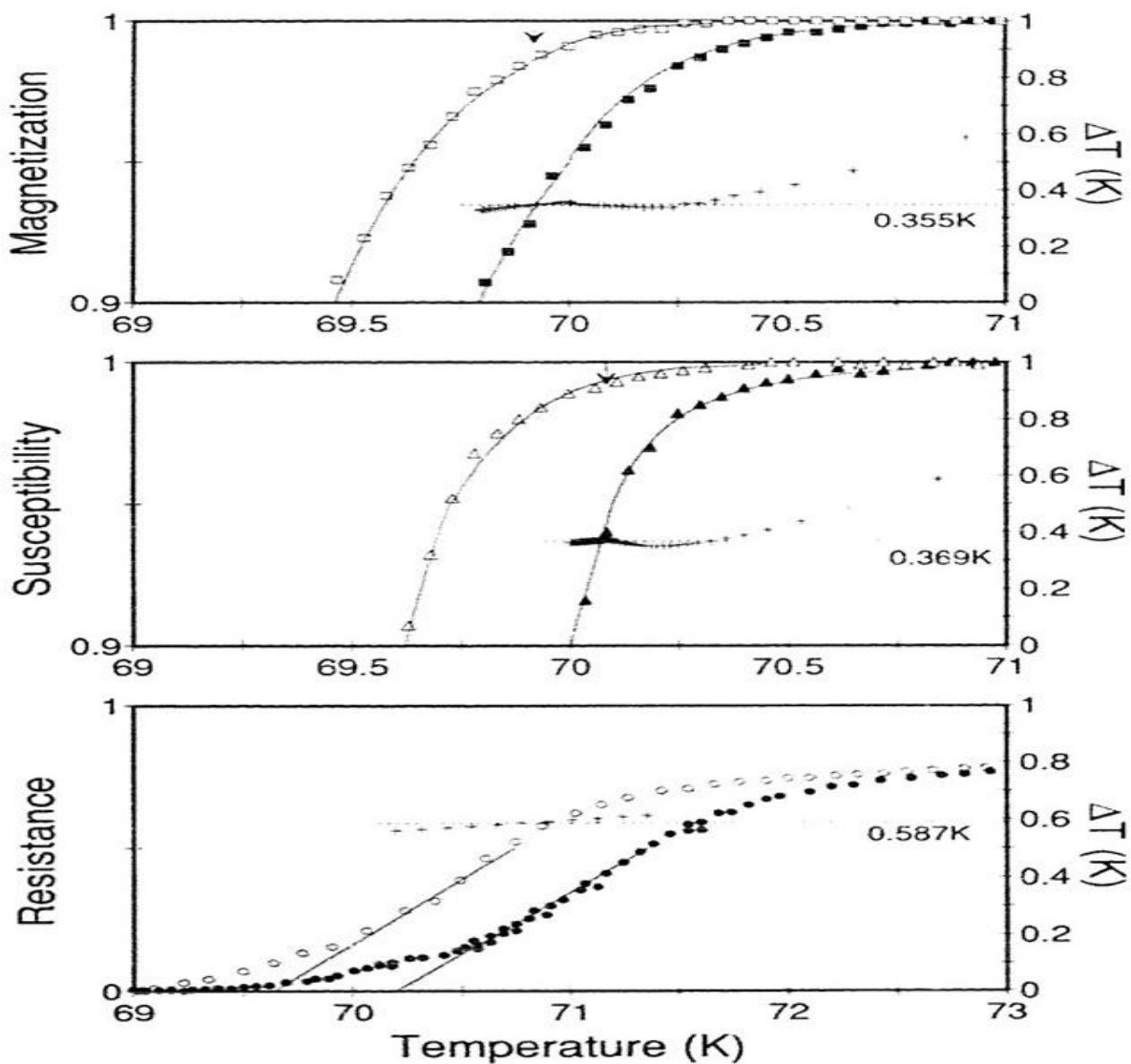


Figure 11 Oxygen isotope effect in $(Y_{0.55}Pr_{0.2}Ca_{0.25})Ba_2Cu_3O_{7-\delta}$, 25% Ca, 20% Pr substitution

Measurement	Sample	$T_c(K)$	$\Delta T_c(K)$	A
dc magnetization	0%	71.0 $\begin{smallmatrix} -2.0 \\ +5.0 \end{smallmatrix}$	0.989 \pm 0.055	0.119 \pm 0.012
	5%	72.5 $\begin{smallmatrix} -0.2 \\ +2.3 \end{smallmatrix}$	0.601 \pm 0.047	0.071 \pm 0.006
	10%	74.2 $\begin{smallmatrix} -0.2 \\ +1.6 \end{smallmatrix}$	0.656 \pm 0.030	0.075 \pm 0.004
	15%	73.0 $\begin{smallmatrix} -0.2 \\ +1.0 \end{smallmatrix}$	0.325 \pm 0.020	0.038 \pm 0.003
	20%	71.4 $\begin{smallmatrix} -0.2 \\ +1.1 \end{smallmatrix}$	0.459 \pm 0.042	0.055 \pm 0.005
	25%	69.9 $\begin{smallmatrix} -0.2 \\ +1.0 \end{smallmatrix}$	0.355 \pm 0.041	0.043 \pm 0.005
ac susceptibility	0%	71.0 $\begin{smallmatrix} -2.0 \\ +5.0 \end{smallmatrix}$	0.968 \pm 0.013	0.117 \pm 0.008
	5%	72.6 $\begin{smallmatrix} -0.2 \\ +2.0 \end{smallmatrix}$	0.565 \pm 0.060	0.066 \pm 0.007
	10%	74.4 $\begin{smallmatrix} -0.2 \\ +1.3 \end{smallmatrix}$	0.661 \pm 0.020	0.074 \pm 0.008
	15%	73.2 $\begin{smallmatrix} -0.2 \\ +0.6 \end{smallmatrix}$	0.324 \pm 0.095	0.040 \pm 0.011
	20%	71.6 $\begin{smallmatrix} -0.2 \\ +1.0 \end{smallmatrix}$	0.482 \pm 0.042	0.057 \pm 0.005
	25%	70.1 $\begin{smallmatrix} -0.2 \\ +1.1 \end{smallmatrix}$	0.369 \pm 0.028	0.045 \pm 0.004
Dc resistance	0%	70.0 $\begin{smallmatrix} -0.3 \\ +0.3 \end{smallmatrix}$	0.969 \pm 0.028	0.118 \pm 0.004
	5%	74.1 $\begin{smallmatrix} -0.1 \\ +0.1 \end{smallmatrix}$	0.600 \pm 0.082	0.073 \pm 0.010
	10%	75.0 $\begin{smallmatrix} -0.3 \\ +0.1 \end{smallmatrix}$	1.000 \pm 0.010	0.111 \pm 0.002
	15%	73.6 $\begin{smallmatrix} -0.1 \\ +0.1 \end{smallmatrix}$	0.486 \pm 0.011	0.059 \pm 0.001
	20%	72.1 $\begin{smallmatrix} -0.2 \\ +0.1 \end{smallmatrix}$	0.575 \pm 0.002	0.071 \pm 0.003
	25%	70.2 $\begin{smallmatrix} -0.7 \\ +0.1 \end{smallmatrix}$	0.587 \pm 0.048	0.072 \pm 0.006

ΔT_c and α vs. T_c for Ca substituted Y(20% Pr)BCO. The positive error bars in temperature reflect the length of the tails in the magnetic measurements. Due to the temperature range platted, the error bars appear, erroneously, larger than that of the previous Pr data.

The filled symbols are the Pr:Ca data while the empty symbols are the 20% Pr samples from the Pr data and are included for comparison.

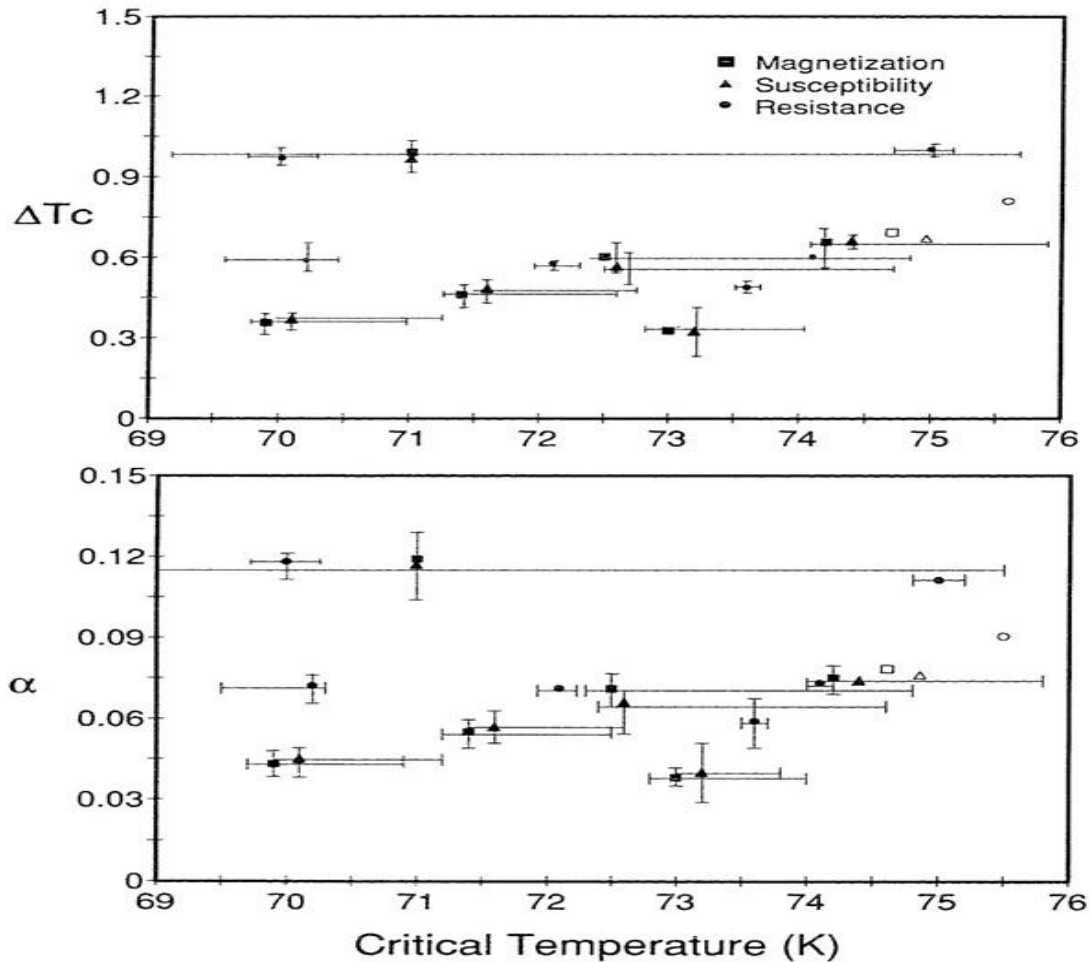


Figure 12

DISCUSSION

The fit of T_c to the concentrations of Pr, x , and Ca, y , to equation [2.1] fit very well. The maximum obtainable T_{c0} (in the YBCO

system) from our calculations is 93.6K, which appears to be a more reasonable value than Neumeier's 97K⁵⁹. We obtain an effective valence of +3.874 for the Pr, slightly smaller than Neumeier's +3.95, which

is consistent with the measurements that indicate a mixed valence between +3 and +4. With the optimum hole concentration, γ ($= 0.091$) being slightly smaller than Neumeier's ($\gamma = 0.1$), the predicted (relative) change in mobile hole concentration will also be very similar. In fact, only one parameter is significantly different from Neumeier's, and that is the coefficient A. Our value of $A = 157\text{K}$ is 37% of Neumeier's $A = 425\text{K}$. The smaller value of A suggests that T_c would be more strongly affected by pair-breaking than by a change in hole concentration. The 20% Pr, 0% Ca sample made for comparison, is quite different from that of the Pr20-50% system. Its T_c is about 5K lower than before, the magnetic transition width is much

broader (-1.4X) and its isotope shift is also larger (-1.5X). Clearly the preparation technique greatly affects the characteristics and hence the quality of the samples. As the highest quality materials, single crystals, tend to have very sharp transitions, and the polycrystalline materials have broader transitions, the relationship between the isotope shift and the width of the transition was investigated for both the Pr and Pr:Ca substituted materials. A linear correlation between the ΔT_c and the transition width is found. The intercept for a zero-width transition remains finite, in the range of 0.3K to 0.4K. This result poses the question of whether the isotope shift should actually be taken as a constant for this system.

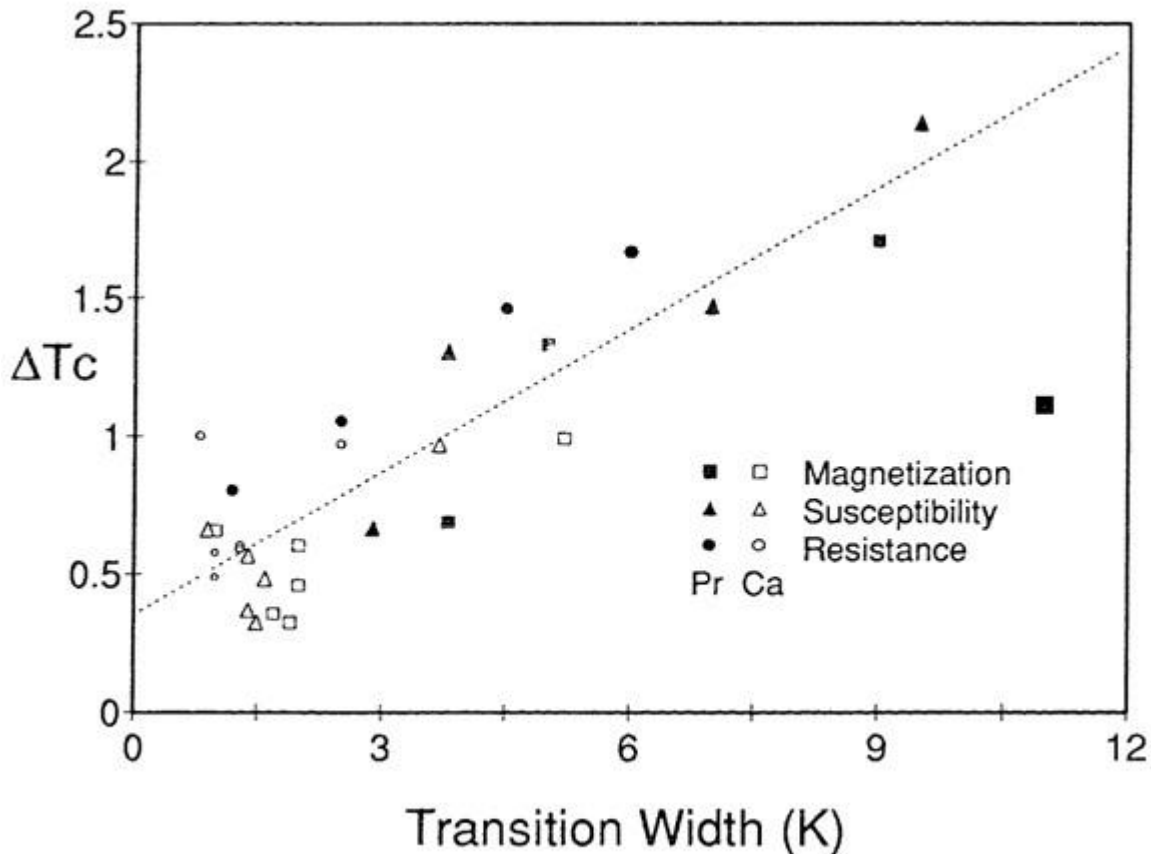


Figure 13

ΔT_c vs. transition width for the Pr and the Pr:Ca system. The dotted line is a linear fit to the data indicates a possible relationship between the magnitude of the isotope shift, ΔT_c , and the width of the transition. In the Pr system, we noted that the tails in the magnetic measurements become much larger with the increase in Pr concentration as do the transition widths, and the isotope shifts. The Ca data with its much sharper transitions and lack of low shielding tails do not exhibit this same effect. As both sets of samples have similar impurity lines in the X-ray data, it is unlikely that the long tails can be attributed solely to the impurities within the samples. Of course, the Ca substitution does not have the large effect on T_c , that the Pr does and it may then be argued that ΔT_c , the transition width, as well as the isotope shift are dependent on T_c .

Conclusion

There does exist, in the high temperature superconducting system of $(y_{1-x}\text{Pr}_x)\text{Ba}_2\text{Cu}_3\text{O}_{7-\delta}$, $(Y_{0.8-y}\text{Pr}_{0.2}\text{Ca}_y)\text{Ba}_2\text{Cu}_3\text{O}_{7-\delta}$ and $\text{YBa}_2(\text{Cu}_{1-z}\text{Zn}_z)\text{O}_{7-\delta}$ an oxygen isotope effect. In all cases, the dc magnetization, the ac susceptibility and the dc resistive measurements show that the substitution of the heavier ^{18}O isotope for ^{16}O leads to a reduction in the critical temperature. For the Pr data, the isotope shift in T_c , ΔT_c increases with increasing concentration; hence α also increases and at the highest concentration is approximately $1/2$. The Zn data has a relatively constant or perhaps even a slightly decreasing ΔT_c , with increasing concentration. Consequently α increases to approximately $1/3$ as T_c , drops.

The critical temperature and isotope coefficient were modeled using a modification to the BCS theory involving a logarithmic Van Hove singularity in the density of states. This model proved relatively successful in that it predicts the general trends found in our data: the small α at the highest T_c , and an increase in α as T_c drops. The range of change for a predicted is reasonable although the actual values are somewhat larger than observed. The response of the VHS model relies heavily on the parameter δ , the difference between the singularity in the DOS and the Fermi energy. The smaller δ becomes, the more the isotope shift is reduced. Thus this model indicates that the difference between the peak in the DOS and the Fermi energy is an important feature.

Reference:

- [1] T.A. Falens, W.K. Ham, S.W. Keller, K.J. Leary, J.N. Michaels, A.M. Stacy, H.C. zur Loye, D.E. Morris, T.W. Barbee III, L.C. Bourne, M.L. Cholen, S. Hoen AND a.Zettl, Phys. Rev. Lett., 59, 915 (1987).
- [2] L. Quan, Y.wei, Q. Yan, G. Chen, P. Zhang, Z. Shen, Y.Ni, Q. Yang, C. Liu, T.Ning, J. Zhao, Y. Shao, S.Han and J. Li, Solid State Comm., 65, 869 (1988).
- [3] B.Batlogg, R.J. Cava, A.Jayaraman, R.B. Van Dover, G.A. Kourouklis, S. Sunshine, D.W. /Murphy. L.W. Rupp, H.S. Chen, A. White, K.T. Short, A.M. Muijsce, and E.A. Rietman, Phys. Rev. Lett., 58., 2333 (1987).

- [4] B. Batlogg, G. Kourouklis, W. Weber, R.J. Cava, A. Jayaram, A.E. White, K.T. Short, L.W. Rupp and E.A. Rietman, *Phys. Rev. Lett.*, 59 912 (1987).
- [5] H.C. zur Loye, K.J. Leary, S.W. Keller, W.K. Ham, J.N. Michaels and A.M. Stacy, *Science*, 238, 1558, (1987).
- [6] K.J. Leary, H.C. zur Loye, S.W. Keller, W.K. Ham, J.N. Michaels and A.M. Stacy, *Phys. Rev. Lett.*, 59, 1236 (2001).
- [7] D.E. Morris, R.M. Kuroda, A.G. Markeiz, J.H. Nickel and J.Y.T. Wei, *Phys. Rev. B*, 37, 5936 (2016).
- [8] S. hoen, W.N. Creage, L.C. Bourne, M.F. Crommie, T.W. Barbee III, M.L. Cohen and A. Zetti, *Phys. Rev. B*, 39, 2269, (2015).
- [9] H. Katayama- Yoshida, T. Hirooka, A.J. Mascarenhas, Y. Okabe, T. Takahahsi, T. Sasaki, A. Ochiai, T. Suzuki, J.I. Pankove, T.F. Cizek and S.K. Deb, *Jpn. J Appl. Phys.*, 26, L2085 (2002).
- [10] H. Katayama- Yoshida, T. Hirooka, A.J. Mascarenhas, Y. Okabe, T. Takahahsi, T. Sasaki, A. Ochiai, T. Suzuki, J.I. Pankove, T.F. Cizek and S.K. Deb, R.B. Goldfarb and Y. Li, *Physica C*, 156, 481 (1988).
- [11] M.K. Crawford, M.N. Kunchur, S.J. Poon, *Phys. Rev. B*, 41, 282 (2004).
- [12] H.J. Bornemann and D.E. Morris, *Phys. Rev. B*, 44, 5322, (1991).
- [13] A.I. Kingon, S. Chevacharoenkul, S. Pejovnik, R. Velasquez, R. Porter, I. Hare and H. Palmour, *High Temperature Superconducting Materials*, editors W. E. Hatfield and J.H. Miller, Marcel Dekker Inc., New York, 327 (1988)
- [14] C.C. Tsuei, *Physica A*, 168, 238, (2005).
- [15] J.S. Sheir and D.M. Ginsberg, *Phys. Rev.*, 147, 384 (1966).
- [16] P.P. Frietas, C.C. Tsuei and T.S. Plaskett, *Phys. Rev. B*, 36, 833 (1987).
- [17] B. Oh, K. Char, A.D. Kent, M. Naito, M.R. Beasley, T.H. Geballe, R.H. Hammond, A. Kapitulnik, J.M. Graybeal, *Phys. Rev. B*, 37, 7861 (1988).
- [18] D- Chen, J-A, Brug, and R. B. Goldfarb, *IEEE Transactions on Magnetics*, 27, 3601 (1991).
- [19] M. Denhoff, S. Gyax and J.R. Long, *Cryogenics*, July, 400 (2003).
- [20] R.B. Goldfarb, M. Lental, C.A. Thompson, *Alternating-Field Susceptometry and Magnetic Susceptibility of Superconductors*, *Magnetic Susceptibility of Superconductors and Other Spin Systems*, editors R.A. Hein, T.L. Francavilla and D.H. Liebenberg, Plenum Press, New York, 49 (1992).



- [21] J.D. Jorgensen, B.W. Veal, A.P. Paulikas, L.J. Nowicki, G.W. Crabtree, H. Claus and W.K. Kwok, Phys. Rev. B, 41,1863 (1990).
- [22] Y- Ueda and K. Kosuge, Physica C,156,281 (2005).
- [23] R.J. Cava, B. Batlogg, C.H. Chen, E.A. Rietman, S.M. Zahurak and D. Werder, Phys. Rev. B, 36, 5719 (1987); Nature, 329, 423 (1987).
- [24] F. Beech, S. Miraglia, A. Santoro and R.S. Roth, Phys. Rev. B, 35, 8778 (1987).
- [25] K.A. Muller, ZPhys. B,80,193(1990).
- [26] B.W Veal, A.P. Paulikas, H. You, H. Shi, Y. Fang and J.W. Downey, Phys. Rev. B, 42,6305 (1990).
- [27] J.L. Tallon and N.E. Flower, Physica C, 204,237 (2006).
- [28] J.P. Franck, J. Jung, G. Salomons, W.A. Miner, M.A.K. Mohamed, J. Chrzanowski, S. Gygax, J.C. Irwin, D.F.Mitchell and G.I. Sproule, Physica C, 172, 90(2006).
- [29] KC. Ott, J.L. Smith, J.O. Willis, R. M. Aikin, E. Garcia, M. Goldblatt, W.B. Hutchinson, G.H. Kwei, C.B. Pierce, J.F. Smith, J.D. Thompson and T.E. Walker, Los Alamos National Laboratory, unpublished work, (2009).
- [30] P.J. Yvon, R.B. Schwarz, C.B. Pierce, L. Bernardez, A. Connor and R. Melsenheimer, Phys. Rev. B, 39, 6690 (1989).